Colloids and Surfaces B: Biointerfaces 194 (2020) 111194

Contents lists available at ScienceDirect

Colloids and Surfaces B: Biointerfaces

journal homepage: www.elsevier.com/locate/colsurfb

Understanding how natural sequence variation in serum albumin proteins affects conformational stability and protein adsorption

Gamaliel Junren Ma[a], Abdul Rahim Ferhan[a], Tun Naw Sut[a,b], Joshua A. Jackman[b,*], Nam-Joon Cho[a,*]

[a] School of Materials Science and Engineering, Nanyang Technological University, 50 Nanyang Avenue, 639798, Singapore
[b] School of Chemical Engineering, Sungkyunkwan University, Suwon, 16419, Republic of Korea

ARTICLE INFO

Keywords:
Bovine serum albumin
Human serum albumin
Rat serum albumin
Protein adsorption
Conformational stability

ABSTRACT

Serum albumins are evolutionary conserved proteins that are found in many animal species, and purified forms are widely used in biotechnology applications, such as components within surface passivation coatings and drug delivery systems. As such, there has long been interest in studying how serum albumins adsorb onto solid supports, although existing studies are limited to one or two species. Herein, we comprehensively investigated three serum albumins of bovine (BSA), human (HSA), and rat (RSA) origin, and discovered striking differences in their conformational stabilities and adsorption properties. Together with bioinformatics analysis, dynamic light scattering (DLS) and circular dichroism (CD) spectroscopy measurements revealed that the proteins form different types of macromolecular assemblies in solution. BSA and HSA existed as individual monomers while RSA formed multimers, and each protein exhibited sequence-dependent variations in conformational stability as well. Quartz crystal microbalance-dissipation (QCM-D) and localized surface plasmon resonance (LSPR) experiments further showed that BSA and HSA proteins adsorb to form well-packed adlayers, and the extent of protein uptake and spreading depended on their unique conformational stabilities. Conversely, RSA adsorption resulted in sparse adlayers and appreciably less spreading of the adsorbed multimers, as confirmed by attenuated total reflection Fourier-transform infrared (ATR-FTIR) spectroscopy experiments. Together, our findings demonstrate that significant differences in conformational stability and adsorption behavior exist even between evolutionary conserved serum albumins with high sequence and structural similarity and illustrate how rational engineering of protein structures and stabilities, guided by insights from nature, might be useful to design protein-based coatings for various biointerfacial science applications.

1. Introduction

There is broad interest in studying protein adsorption at solid-liquid interfaces [1], which is important for fundamental biointerfacial science as well as for applications such as medical implants [2], biosensors [3], and bionanotechnology tools [4]. Over the years, a wide range of model protein systems have been studied and perhaps the most important one is the class of serum albumin proteins that are found in the vertebrate blood of various mammals, are naturally abundant, and well-characterized in terms of fractionation methods for extraction [5,6]. Certain species are also widely used as surface passivation ("blocking") agents in molecular biology and biotechnology applications [7–9].

One important factor affecting the adsorption behavior of serum albumins, and proteins in general, is the conformational stability of a protein in the solution phase. A protein will naturally fold into the most energetically stable structure that is kinetically accessible, and a protein with greater conformational stability (*i.e.*, due to stronger intramolecular forces) will prefer to remain in that state and adsorption can be less favorable in such cases. On the other hand, proteins with lower conformational stability typically have weaker intramolecular forces that hold together the folded protein structure, leaving protein molecules more prone to unfold and denature upon adsorption due to protein-surface interactions [10]. A key factor influencing conformational stability is the primary amino acid sequence of a protein and corresponding effects on the folded structure. To date, this factor has been explored using engineered proteins with rationally inserted amino acid mutations to either increase or decrease conformational stability and to evaluate the effects on protein adsorption accordingly. Karlsson et al. first demonstrated the relationship between protein structure, conformational stability, and adsorption behavior by using several

* Corresponding authors.
E-mail addresses: jjackman@skku.edu (J.A. Jackman), njcho@ntu.edu.sg (N.-J. Cho).

https://doi.org/10.1016/j.colsurfb.2020.111194
Received 16 March 2020; Received in revised form 2 June 2020; Accepted 11 June 2020
Available online 13 June 2020

engineered versions of the carbonic anhydrase II protein [11]. The results showed greater adsorption irreversibility for engineered proteins with lower conformational stability in the solution phase.

While protein engineering enables the systematic investigation of specific amino acid mutations, it is also interesting to profile the conformational stability of naturally occurring, structurally related proteins in order to determine effects on adsorption properties, and serum albumins from different species provide an ideal option. Indeed, serum albumins from different species share certain physicochemical features [12,13] and similar three-dimensional crystal structures [14–16], but there are also differences in solution properties such as ligand binding [17–24], which provides motivation to investigate how structural variations in serum albumin proteins can affect their conformational stability and adsorption behavior. So far, there have been reports that serum albumins from bovine, human, rat, dog, rabbit, and pig species exhibit unique characteristics related to solution-phase conformational stability, such as thermal denaturation profile [25–28]. However, a comparative evaluation of the adsorption behavior of different serum albumin species and how such properties are linked with conformational stability is lacking and the adsorption properties of bovine and human serum albumins have been the only ones tested [29–36].

Herein, we experimentally investigated bovine serum albumin (BSA), human serum albumin (HSA), and rat serum albumin (RSA), to understand the interplay between naturally occurring sequence variations and corresponding effects on adsorption. Using a bioinformatics approach, we first conducted amino acid sequence comparisons followed by experimental characterization of each protein's solution-phase conformational stability, real-time adsorption behavior, and adsorption-related conformational changes. Collectively, our findings build a mechanistic picture of how sequence variations in BSA, HSA, and RSA proteins affect adsorption behavior and the resulting insights can also guide the engineering of proteins with modulated conformational stabilities for fabricating adsorbed protein layers as biointerfaces.

2. Materials and methods

2.1. Reagents

Bovine serum albumin (BSA, A7030, lot no. SLBT4132), human serum albumin (HSA, A3782, lot no. SLBN5035V), rat serum albumin (RSA, A6414, lot no. SLBQ0209V), sodium dodecyl sulfate (SDS, L4390), and sodium chloride (NaCl, 746398) were purchased from Sigma-Aldrich (USA). Tris(hydroxymethyl)aminomethane (Tris, 0497) was purchased from Amresco (USA). Ethanol (95 %) was purchased from Aik Moh (Singapore), and hydrochloric acid (100317) was purchased from Merck (USA).

2.2. Sample preparation

Buffer solutions were prepared to 10 mM Tris, 150 mM NaCl, and pH 7.5 in Milli-Q-treated water ($> 18.2\,M\Omega\,cm$, 25 °C) and filtered through a 0.2 μm filter (595–4520 Thermo Scientific, USA). All protein solutions were prepared by dissolving lyophilized powders in buffer solution and then filtering through a 0.2 μm syringe filter (PN-4612, Pall Corporation, USA). The molar concentrations of BSA, HSA, and RSA proteins in aqueous buffer solution were determined by ultraviolet light absorbance measurements at 280 nm using molar extinction coefficient values of 42,925, 34,445, and 38,915 $M^{-1}\,cm^{-1}$ respectively [37].

2.3. Dynamic light scattering

Intensity-weighted size distributions of 150 μM BSA, HSA, and RSA proteins were determined by dynamic light scattering (DLS) measurements (ZetaPALS, Brookhaven Instruments, USA) and analyzed by the Particle Solutions software (Brookhaven Instruments). Temperature-dependent measurements were first recorded at 25 °C, and then from 50 to 75 °C in 5 °C increments. A 5-min equilibration was conducted after each temperature increment. Time-dependent measurements were conducted by maintaining the temperature at 60 °C and taking size measurements every 10 min for 200 min. All reported values were obtained from 5 measurements. DLS characterization was conducted to measure the size distribution of the protein samples prior to all experiments. The standard deviation (s.d.) related to the size distribution of the protein samples was obtained by dividing the full-width-at-half-maximum (FWHM) of the Gaussian size distribution from DLS measurements by $2\sqrt{2\ln 2} \approx 2.355$.

2.4. Circular dichroism spectroscopy

Temperature-dependent circular dichroism (CD) spectroscopy measurements were conducted in a similar format to DLS experiments. Measurements were taken in triplicate and all the sample spectra were subtracted by a background buffer spectrum. More details are provided in Supplementary Material.

2.5. Quartz crystal microbalance-dissipation

Protein adsorption kinetics on silica-coated sensor surfaces were characterized by quartz crystal microbalance-dissipation (QCM-D) experiments conducted using the QSense E4 instrument (Biolin Scientific AB, Sweden) with silica-coated quartz crystal sensor chips (QSX 303, Biolin Scientific). Before each experiment, the sensor chips were washed by sequentially rinsing with 1 % (wt/vol) aqueous SDS solution, water, and ethanol. After drying under a gentle stream of nitrogen gas and oxygen plasma treatment (PDC-002, Harrick Plasma, USA) for 3 min, the chips were assembled into the measurement chamber. For experiments, liquid samples were injected into the measurement chamber at a flow rate of 100 μL/min. A stable baseline was first established with buffer solution, then 50 μM protein samples were injected for 30 min, followed by a buffer washing step. All measurements were conducted at 25 °C. The corresponding resonance frequency (ΔF) and energy dissipation (ΔD) shifts were recorded in real-time at multiple odd overtones, as previously described [38]. Data collected at the fifth overtone are reported. Measurement operations were controlled by the QSoft 401 (Biolin Scientific) software package.

2.6. Localized surface plasmon resonance

Ensemble-averaged localized surface plasmon resonance (LSPR) experiments were conducted to characterize the adsorption behavior of the protein samples onto silica-coated sensor chips containing gold nanodisk arrays using an Insplorion XNano instrument (Insplorion AB, Sweden), as previously described [39]. Sensor chip preparation and adsorption experiments were conducted in a similar format to the QCM-D experiments. The Insplorer software package (Insplorion AB) was used to record shifts in the LSPR centroid (peak) position ($\Delta\lambda$) from the extinction spectrum. The rate of change of the $\Delta\lambda$ shifts was determined by calculating the first derivative with respect to time ($d\Delta\lambda/dt$) (see Ref. [40]) by using the OriginPro 2019b software package.

2.7. Attenuated total reflection Fourier-transform infrared spectroscopy

Attenuated total reflection Fourier-transform infrared (ATR-FTIR) spectroscopy experiments were conducted to determine the secondary structure of 100 μM serum albumin proteins in solution and in the adsorbed state. More details are provided in Supplementary Material.

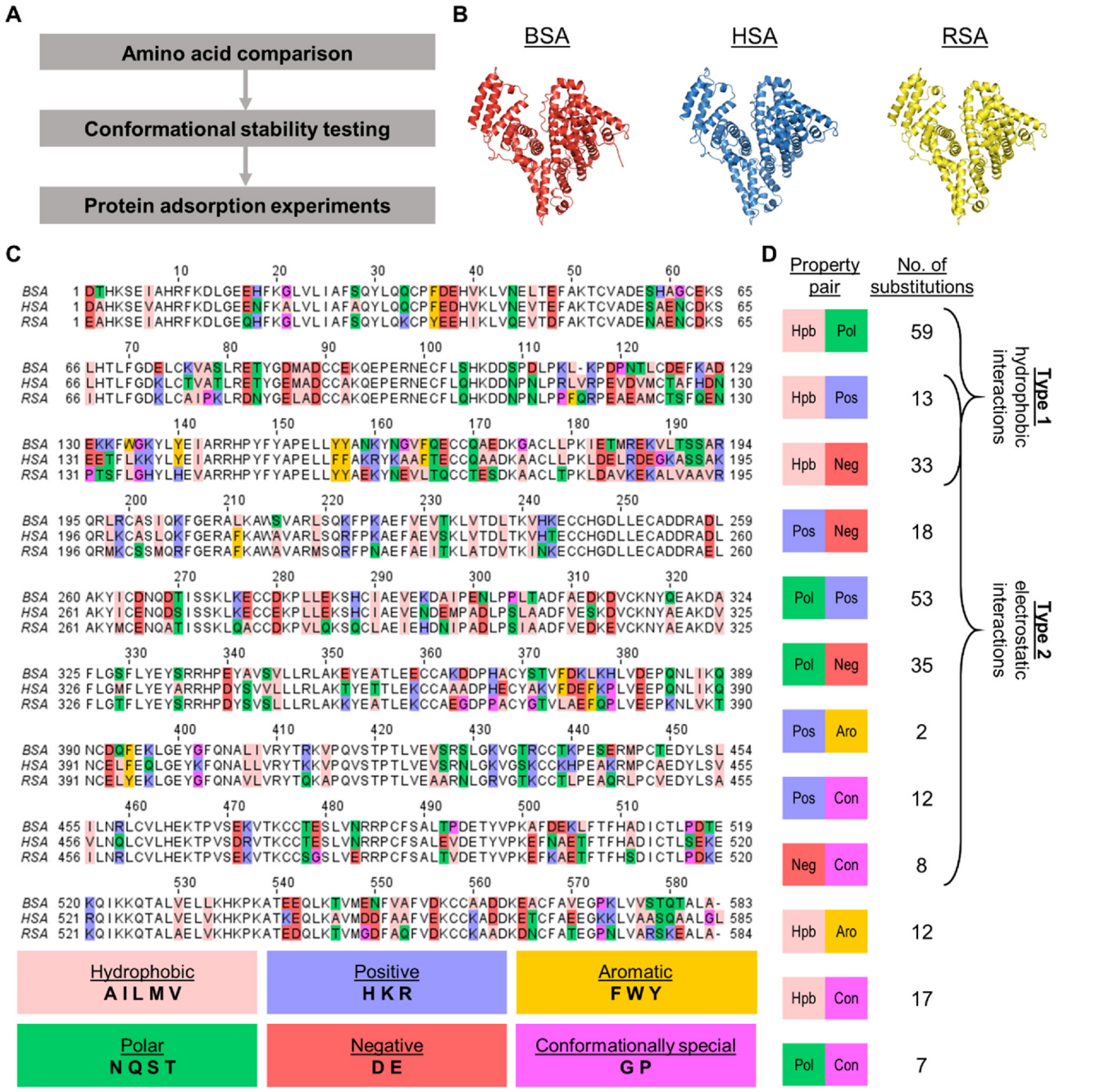

Fig. 1. (A) Experimental strategy to characterize how structural variations between serum albumin proteins affect conformational stability and adsorption behavior. (B) Modeled 3D structures of BSA, HSA, and RSA. (C) Multiple sequence alignment of BSA, HSA, and RSA. Amino acids are classified based on their physicochemical properties according to the Zappo color scheme. (D) List of different physicochemical property pairs and respective number of amino acid substitutions between BSA, HSA, and RSA. Substitutions involving changes in hydrophobic interactions and electrostatic interactions were designated as Type 1 and Type 2, respectively.

3. Results and discussion

3.1. Comparing the amino acid sequences between serum albumin species

We first compared the amino acid sequences of BSA, HSA, and RSA proteins to identify regions of variation that might impact protein conformational stability, followed by experimental characterization of protein conformational stability and adsorption behavior (Fig. 1A). We selected BSA, HSA, and RSA as naturally occurring structural variants of serum albumin proteins. From their 3D model structures, it can be observed that certain similarities exist between the three proteins along with subtle distinctions (Fig. 1B). One possible source of distinction would be the different numbers of positively (R & K) and negatively (D & E) charged residues, amounting to predicted net charges of −17, −15, and −12 for BSA, HSA, and RSA, respectively, which could affect protein conformational stability [41].

To further analyze their sequence differences, a multiple sequence alignment for BSA, HSA, and RSA was plotted (Fig. 1C). The Zappo color scheme helps to identify sequence variations with different physicochemical properties. Such variations could indicate different extents of intramolecular interactions (hydrophobic, electrostatic, and hydrogen bonding) which directly affect protein conformational stability [41,42]. Since certain substitutions occur between residues under the same physicochemical classification, we listed different physicochemical property pairs and their respective number of substitutions and in doing so, identified two types of substitutions that were most likely to

affect protein conformational stability: (1) hydrophobic/polar and hydrophobic/charged substitutions that lead to changes in hydrophobic interaction propensity; and (2) neutral/charged substitutions and substitutions between oppositely charged residues that lead to changes in electrostatic interactions (Fig. 1D). Type 1 substitutions comprise almost 40 % of all substitutions while Type 2 substitutions were around 60 %. These analyses indicate that the three proteins likely have different conformational stabilities on account of variations in amino acid sequence that influence hydrophobic and electrostatic interactions vis-à-vis protein-surface and protein-protein interactions.

3.2. Solution-phase conformational stability of serum albumin proteins

We then measured the solution-phase conformational stability of each serum albumin by conducting temperature-dependent dynamic light scattering (DLS) and circular dichroism (CD) spectroscopy experiments. The onset temperature of oligomerization was determined by recording the lowest temperature at which an appreciable increase in protein size was observed. CD spectroscopy measurements were conducted to determine the extent of thermal unfolding as indicated by changes in secondary structure.

The measured sizes of BSA, HSA, and RSA at 25 °C were 9.4, 8.1, and 28.7 nm, respectively, indicating that BSA and HSA exist as monomers while the larger size of RSA suggests that it is present either as irreversibly denatured oligomers [36,43] or as non-denatured multimers [44] (Figs. 2A & S1). In all cases, no temperature-induced oligomerization was observed at 50 and 55 °C as the sizes of the three serum albumins remained constant up to this temperature range. By contrast, at 60 °C, the sizes of BSA, HSA, and RSA proteins were 12.8, 8.2, and 34.1 nm, respectively, while at 65 °C, their sizes were 23.8, 12.4, and 33.2 nm, respectively. These data indicate that BSA oligomerization occurred at 60 °C, which is consistent with our previous work [35], while HSA oligomerization occurred at a higher temperature of 65 °C. This finding supports that HSA is more stable against temperature-induced oligomerization than BSA. Time-dependent experiments further verified that BSA underwent more extensive oligomerization than HSA (Fig. S2). Conversely, RSA displayed temperature-induced oligomerization behavior at 70 °C, reaching 184.6 nm. In both temperature-dependent and time-dependent DLS measurements, RSA exhibited a slight decrease in size prior to oligomerization. This is likely due to temperature-induced unfolding and reconfiguration of its constituent monomers to form more compact denatured oligomers. Interestingly, at 70 °C, HSA achieved a larger mean size of 65.7 nm compared to 34.3 nm for BSA despite having a higher onset temperature of oligomerization. At 75 °C, HSA and RSA protein oligomerized to micron-scale sizes, which were about two orders of magnitude larger than BSA protein aggregates.

We next conducted CD spectroscopy measurements to determine the percentage of α-helical secondary structure in each protein as a function of temperature (Figs. 2B & S3). CD spectroscopy measurements showed that, at 25 °C, BSA, HSA, and RSA had helicity percentage values of 62.3, 61.8, and 60.2 % respectively, indicating that all serum albumins have high levels of secondary structure and were not denatured [36,43,45]. Taken together, the DLS and CD spectroscopy measurements at 25 °C support that RSA is multimeric, consisting of clustered non-denatured monomers. The multimeric configuration of RSA proteins might relate to its lower net charge than BSA and HSA as mentioned above, which could facilitate more extensive protein-protein interactions.

At higher temperatures, all three proteins underwent thermally induced unfolding, which is observed by a decrease in α-helical percentage at each temperature increment. Serum albumins underwent reversible unfolding at lower temperatures while the folding became irreversible at higher temperatures [27]. In order to take into account the latter, which is usually related to temperature-induced oligomerization, we compared the mean α-helical percentage values at 65 °C, which showed that BSA had the lowest mean α-helical percentage value of 48.8 %, followed by RSA with 49.0 % and HSA with 51.9 %. This trend continued at 70 °C with BSA, RSA, and HSA having values of 41.8 %, 42.3 %, and 43.5 %, respectively, which indicates that BSA underwent the most extensive thermally induced unfolding, followed by RSA and then HSA. At 75 °C, all three serum albumins had similar helicity values despite HSA and RSA displaying more extensive oligomerization than BSA, as indicated by the DLS experiments. Therefore, the DLS and CD spectroscopy data indicate that, while BSA had the lowest onset temperature of oligomerization and most extensive thermal unfolding, BSA also formed the smallest protein aggregates. These data support that BSA has lower conformational stability but greater colloidal stability than HSA and RSA. In other words, HSA and RSA have higher onset temperatures of oligomerization, but oligomerize more

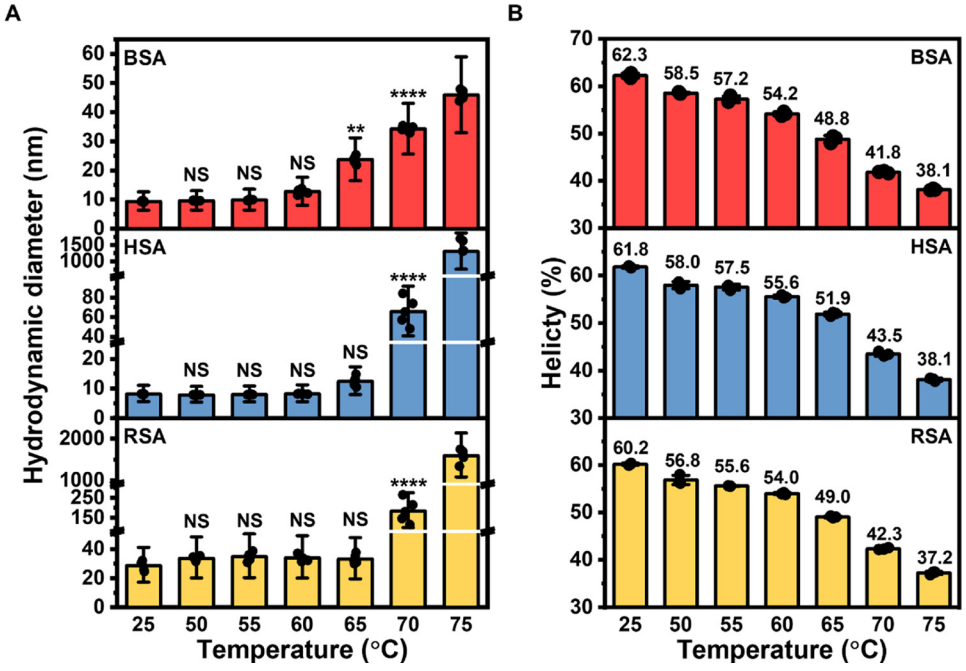

Fig. 2. (A) Hydrodynamic diameter of BSA, HSA, and RSA measured by dynamic light scattering (DLS) as a function of temperature. Data are presented as mean ± standard deviation (s.d.) [n = 5 technical replicates, one-way analysis of variance (ANOVA) with Dunnett's multiple comparisons test (versus data at 25 °C)]. (B) α-helical percentage of BSA, HSA, and RSA as a function of temperature from circular dichroism (CD) spectroscopy experiments. Data are reported as mean ± s.d. (n = 3 technical replicates). Mean values are presented on top of each column.

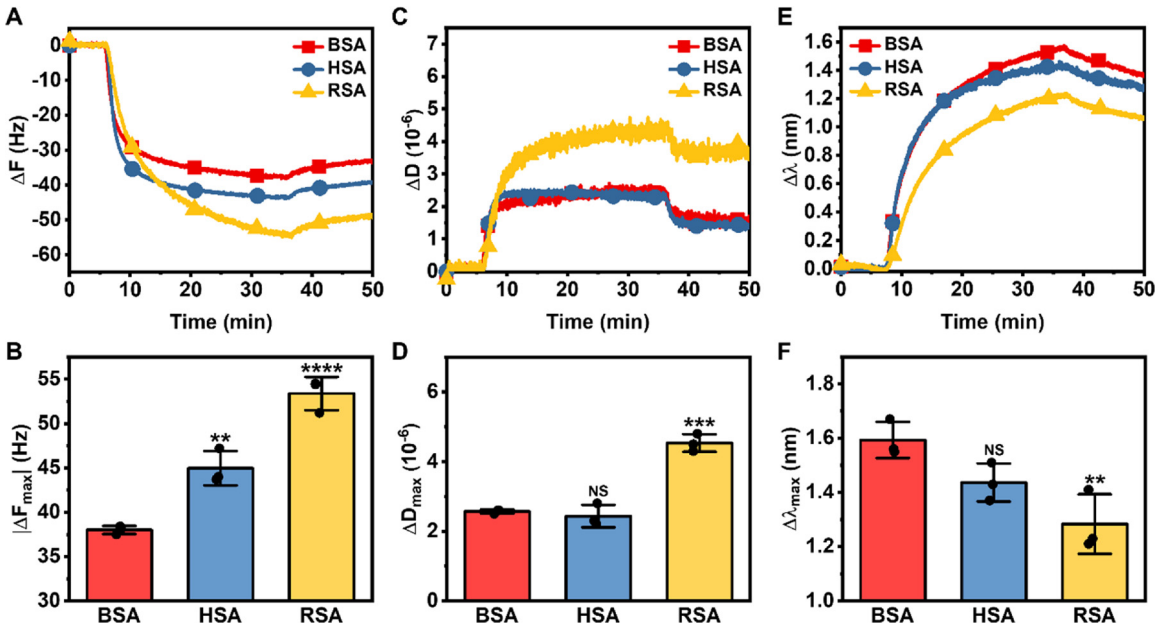

Fig. 3. (A) Time-resolved QCM-D ΔF shifts and (B) corresponding $|\Delta F_{max}|$ values at adsorption saturation. (C) Time-resolved QCM-D ΔD shifts and (D) corresponding ΔD_{max} values at adsorption saturation. (E) Time-resolved LSPR Δλ shifts and (F) corresponding $\Delta\lambda_{max}$ shifts at adsorption saturation. Data in (B), (D), and (F) are presented as mean ± s.d. (n = 3 biological replicates, one-way ANOVA with Tukey's multiple comparisons test). Test results are reported for HSA and RSA (versus BSA). Dots represent individual data points.

extensively to form larger aggregates than those of BSA once unfolded. Collectively, both DLS and CD experiments show that BSA has the lowest solution-phase conformational stability while HSA has the highest, which agrees with the DLS data and other methods [25–27].

3.3. Comparing the adsorption behavior of serum albumin proteins

We next characterized the adsorption behavior of the serum albumins on hydrophilic silica surfaces by using the quartz crystal microbalance-dissipation (QCM-D) technique. The QCM-D resonance frequency shift (ΔF) corresponds to the mass of the adsorbed protein molecules, including hydrodynamically-coupled solvent, while the energy dissipation shift (ΔD) corresponds to the viscoelasticity of the adsorbed film. Larger ΔF shifts typically indicate more adsorption uptake. At adsorption saturation, the adsorption uptake of BSA, HSA, and RSA in terms of mean absolute final frequency shift ($|\Delta F_{max}|$) was 38.0, 45.0, and 53.4 Hz, respectively (Fig. 3A, B). The corresponding mean dissipation shifts (ΔD_{max}) were 2.6, 2.4, and 4.5 × 10^{-6}, respectively (Fig. 3C, D). The higher $|\Delta F_{max}|$ of HSA vs. BSA supports that more HSA monomers adsorbed onto the silica surface while similar ΔD_{max} values were also recorded. Conversely, the larger $|\Delta F_{max}|$ and ΔD_{max} values from the adsorption of multimeric RSA proteins indicates the formation of a thicker and more viscoelastic layer on the silica surface. Further analysis of time-independent F-D curves showed that the BSA and HSA curves have similar gradients and thus form similarly rigid adlayers (Fig. S4). By contrast, RSA's F-D curve yielded a steeper gradient (greater increase in energy dissipation per change in frequency), supporting that RSA multimers form less rigid adlayers than BSA and HSA monomers.

To corroborate the QCM-D adsorption results, we next conducted localized surface plasmon resonance (LSPR) experiments to track protein adsorption onto silica-coated gold nanodisk arrays. Unlike the acoustic-based QCM-D technique, the LSPR platform is optical-based and does not take into account hydrodynamically-coupled solvent mass, only the protein mass itself [46–48]. LSPR measurements also have greater surface sensitivity because of the technique's much shorter sensing depth of < 20 nm compared to ~200 nm in QCM-D measurements [49], and therefore yields a higher signal response when an adsorbed protein undergoes more extensive deformation-related spreading and is thus, on average, closer to the sensor surface [47]. LSPR extinction peak shifts (Δλ) were recorded in real time to track the adsorption of the three serum albumins (Fig. 3E). At adsorption saturation, BSA, HSA, and RSA yielded mean $\Delta\lambda_{max}$ shifts of 1.59, 1.44, and 1.28 nm, respectively (Fig. 3F). Interestingly, this trend is directly opposite of the $|\Delta F_{max}|$ trend obtained from the QCM-D experiments and provides insight into the relative degree of protein denaturation on the silica surface.

The findings from both QCM-D and LSPR experiments support that the BSA proteins are, on average, closer to the sensor surface, undergo more surface-induced spreading, and possess a larger adsorption footprint, thereby reducing the total number of adsorbed BSA molecules on the sensor surface compared to the HSA case. Regarding RSA adsorption behavior, the comparatively smaller LSPR Δλ shift indicates that the entire RSA multimer is detected by the QCM-D platform but only partially detected by the LSPR platform's shorter sensing depth, and that adsorbed RSA molecules are, on average, farther away from the sensor surface and have less dense packing, due to larger-sized RSA multimers having a lower probability of adsorbing between gaps in the pre-adsorbed layer, according to the random sequential adsorption model [50]. Also, the QCM-D platform detects hydrodynamically-coupled solvent in void gaps, while the LSPR platform does not [51]. Taken together, the combination of QCM-D and LSPR experiments revealed key mechanistic differences between the adsorption behavior and resulting adsorbed film properties of each protein. Particularly, BSA underwent greater spreading than HSA upon adsorption to silica surfaces while RSA multimers were more sparsely adsorbed.

3.4. Adsorption-related conformational changes

We next investigated the adsorption-related conformational changes of each protein by further analyzing the LSPR data. We calculated the rate of change of LSPR peak shift ($d\Delta\lambda/dt$), which correlates with the relative extent of surface-induced protein conformational changes (Fig. 4A) [46–48]. The maximum rate of change ($(d\Delta\lambda/dt)_{max}$) during the initial stage of adsorption was computed and the mean $(d\Delta\lambda/dt)_{max}$ values for BSA, HSA, and RSA adsorption were 0.42, 0.42, and 0.16 nm/

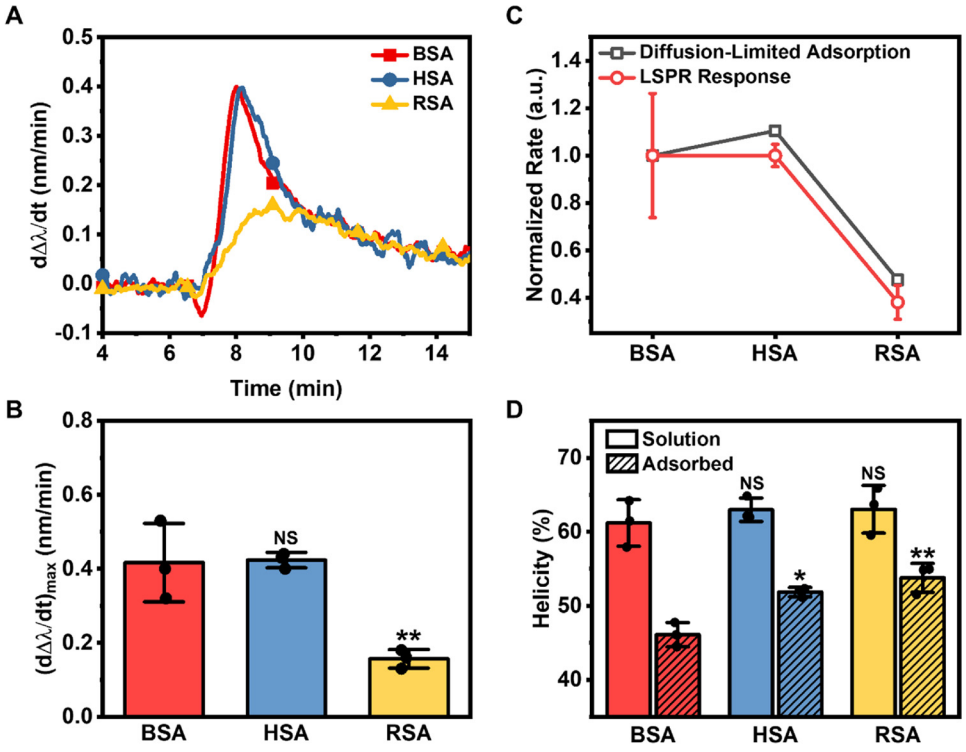

Fig. 4. (A) Rate of change of LSPR peak shift during the initial stage of adsorption ($d\Delta\lambda/dt$) as a function of time and (B) corresponding maximum rate of change of LSPR peak shift during the initial stage of adsorption $(d\Delta\lambda/dt)_{max}$. (C) Comparison between the rate of size-related diffusion-limited adsorption and the maximum rate of change in LSPR peak shift data from (B). Rates are normalized to the BSA case. (D) α-helical percentage of BSA, HSA, and RSA proteins in solution and upon adsorption from ATR-FTIR spectroscopy experiments. Data in (B), (C), and (D) are presented as mean ± s.d. [n = 3 biological replicates, one-way ANOVA in (B) and two-way ANOVA in (D) with Tukey's multiple comparisons test]. Test results in (B) are reported for HSA and RSA (versus BSA). Test results in (D) are reported for HSA and RSA (versus BSA) in solution and are separately reported for HSA and RSA (versus BSA) in the adsorbed state. Dots in (B) and (D) represent individual data points.

min, respectively (Fig. 4B). We note that the experimentally measured rate reflects both the diffusion-limited adsorption and the extent of surface-induced denaturation [47,48]. Since all experiments were conducted in identical environmental conditions, diffusion-limited adsorption would only be affected by the size of the protein samples. To resolve the effects of protein size and surface-induced denaturation on the LSPR rate, we compared the theoretical size-dependent diffusion-limited adsorption rate with the experimentally measured rate (see Supplementary Material), and differences between the two trends can be attributed to differences in surface-induced denaturation. Upon normalizing to the BSA case, the rates were plotted in Fig. 4C and the diffusion-limited rates for HSA and RSA were higher than their measured rates, suggesting that HSA and RSA undergo less surface-induced denaturation than BSA during the initial stage of adsorption.

To corroborate these results, we conducted attenuated total reflection Fourier-transform infrared (ATR-FTIR) spectroscopy experiments to determine the secondary structure of the three serum albumins in the solution state and in the adsorbed state (Fig. S5). The mean α-helical percentage of BSA, HSA, and RSA were 61.2, 63.0, and 63.0 %, respectively, in the solution state, and 46.1, 51.9. and 53.8 %, respectively, in the adsorbed state (Fig. 4D). These results show that BSA experienced a greater loss in α-helical percentage than HSA, supporting previous adsorption data that BSA underwent more extensive surface-induced denaturation upon adsorption and is more spread out than HSA. Conversely, RSA proteins incurred the least extensive loss in α-helicity. Notably, the ATR-FTIR penetration depth is ~1.2 μm [52], indicating that the data reflects the average secondary structure of all the molecules within the RSA multimer and supporting that the molecules in contact with the surface denature while other molecules in the multimer predominately remain in their native state, thereby preventing RSA multimers from deforming as much as BSA and HSA monomers. This supports evidence from the adsorption studies that RSA multimers adsorb with relatively larger interparticle spacing due to its larger size and also due to its restricted ability to spread on the surface.

3.5. Mechanistic picture of BSA, HSA, and RSA protein adsorption behavior

We present an overall mechanistic picture of the adsorption behavior for each serum albumin, including their relationship to solution-phase conformational stability. BSA and HSA in solution exist as individual molecules in their native state (monomers), while RSA in solution exist as composites of native monomers (multimers) (Fig. 5A). Compared to HSA, BSA has lower conformational stability in solution, as observed by BSA having a lower onset of temperature-induced oligomerization and undergoing more extensive temperature-induced conformational changes. Adsorbed BSA proteins have more extensive surface-induced denaturation than HSA and thus more spreading on the surface as well (Fig. 5B). Taken together, our findings demonstrate how natural sequence variations between serum albumins give rise to variations in conformational stability, and surprisingly colloidal organization (monomers vs. multimers) as well, that directly impact the specific adsorption behavior of each protein. In general, the data support that BSA forms tightly packed adlayers consisting of well-spread protein molecules while HSA does so to a lesser extent. Due to its larger size, RSA forms sparser adlayers which are likely less effective as surface passivation coatings.

4. Conclusion

Herein, we compared the conformational stability and adsorption behavior of three different serum albumins, BSA, HSA, and RSA, to unravel how naturally occurring, evolutionary conserved variations in amino acid sequence affect protein structure and consequently influence protein adsorption behaviors. We found that BSA and HSA are monomers in solution, while RSA exists as multimers consisting of helical protein molecules, and the two types of macromolecular assemblies have distinct adsorption behaviors. BSA and HSA adsorbed onto silica surfaces to form a single layer of adsorbed protein molecules and the extent of protein uptake and spreading depended on their conformational stability. Conversely, RSA adsorption resulted in less-dense adlayers because the adsorbing species were multimers and there was less spreading of adsorbed protein molecules within the adlayer

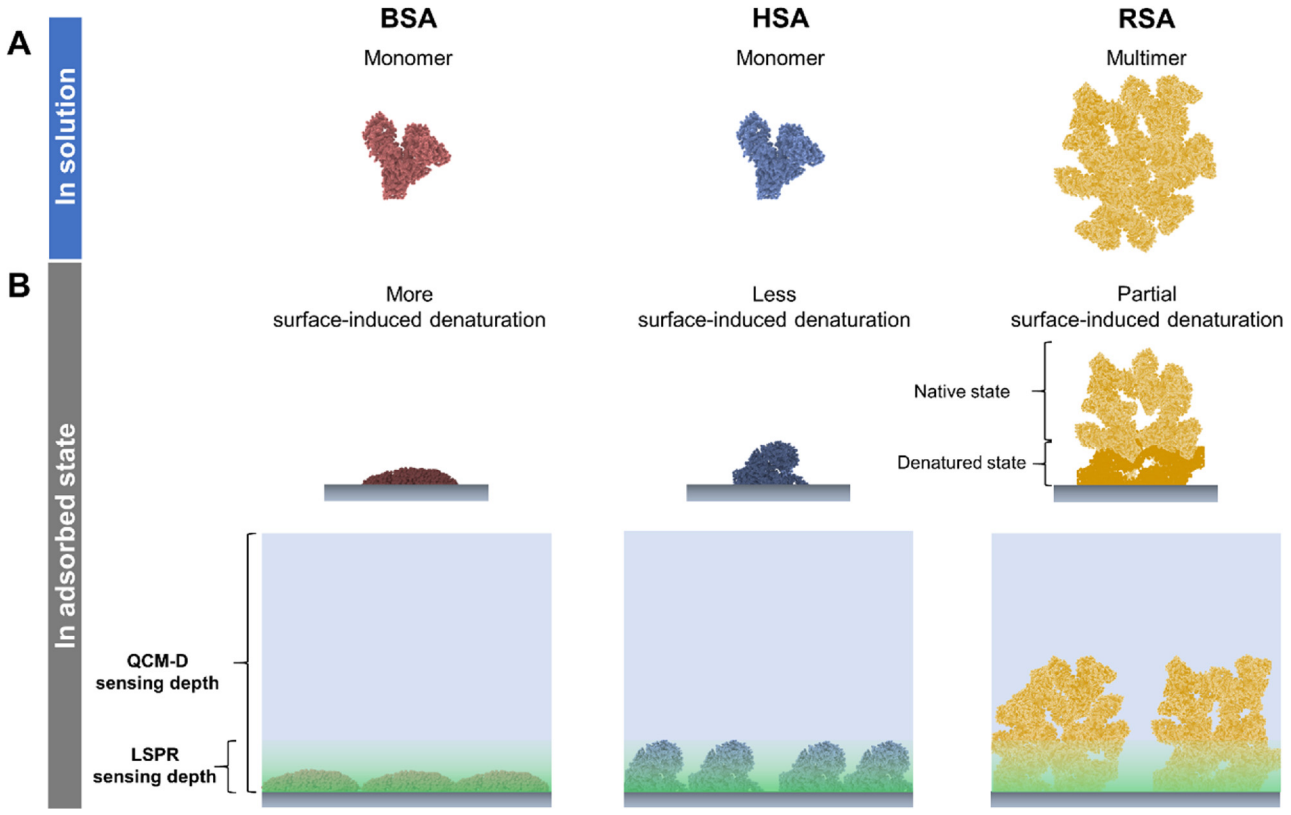

Fig. 5. Schematic illustration of BSA, HSA, and RSA proteins in solution and conformational stability-related adsorption behavior trends. (A) BSA and HSA proteins exist as monomers while RSA proteins are assembled as multimers in solution. (B) BSA, HSA, and RSA display different adsorption behaviors. BSA's lower conformational stability than HSA leads to greater surface-induced denaturation and larger footprint size. Adsorption of larger RSA multimers results in denaturation of only the molecules in contact with the surface (darker colored) while other molecules remain in their native state.

because only some protein molecules within the multimers contacted the surface and were subjected to protein-surface interactions directly. Thus, even with the range of evolutionary conserved serum albumins with high sequence and structural similarity, we observed key differences in conformational stability and adsorption behavior. These findings not only offer fundamental insight into protein adsorption but also provide mechanistic support to explain why, among the serum albumins, BSA is so useful to form surface passivation ("blocking") coatings on solid supports. Our combination of solution-phase and surface-sensitive experiments along with bioinformatics provides an avenue to also engineer serum albumin derivatives and other proteins with programmed conformational stabilities and other physiochemical characteristics (*e.g.*, net charge) to modulate adsorption behaviors and potentially control the formation of protein layers with enhanced application possibilities.

Declaration of Competing Interest

The authors declare that they have no known competing financial interests or personal relationships that could have appeared to influence the work reported in this paper.

CRediT authorship contribution statement

Gamaliel Junren Ma: Conceptualization, Methodology, Investigation, Formal analysis, Writing - original draft, Visualization. **Abdul Rahim Ferhan:** Conceptualization, Methodology, Formal analysis, Visualization. **Tun Naw Sut:** Investigation, Visualization. **Joshua A. Jackman:** Conceptualization, Methodology, Formal analysis, Writing - review & editing, Supervision, Funding acquisition. **Nam-Joon Cho:** Conceptualization, Resources, Supervision, Funding acquisition.

Acknowledgements

This work was supported by the National Research Foundation of Singapore through a Competitive Research Programme grant (NRF-CRP10-2012-07) and a Proof-of-Concept grant (NRF2015NRF-POC0001-19), and by the National Research Foundation of Korea (NRF) grant funded by the Korean government (MSIT) (No. 2020R1C1C1004385).

Appendix A. Supplementary data

Supplementary material related to this article can be found, in the online version, at doi:https://doi.org/10.1016/j.colsurfb.2020.111194.

References

[1] M. Rabe, D. Verdes, S. Seeger, Understanding protein adsorption phenomena at solid surfaces, Adv. Colloid Interface Sci. 162 (2011) 87–106.
[2] S.R. Meyers, M.W. Grinstaff, Biocompatible and bioactive surface modifications for prolonged in vivo efficacy, Chem. Rev. 112 (2011) 1615–1632.
[3] J.S. del Río, O.Y. Henry, P. Jolly, D.E. Ingber, An antifouling coating that enables affinity-based electrochemical biosensing in complex biological fluids, Nat. Nanotechnol. 14 (2019) 1143–1149.
[4] C.D. Walkey, W.C. Chan, Understanding and controlling the interaction of nanomaterials with proteins in a physiological environment, Chem. Soc. Rev. 41 (2012) 2780–2799.
[5] E.J. Cohn, L.E. Strong, W. Hughes, D. Mulford, J. Ashworth, M. Melin, H. Taylor, Preparation and properties of serum and plasma proteins. IV. A system for the separation into fractions of the protein and lipoprotein components of biological tissues and fluids, J. Am. Chem. Soc. 68 (1946) 459–475.
[6] W. Schneider, H. Lefevre, H. Fiedler, L.J. McCarty, An alternative method of large scale plasma fractionation for the isolation of serum albumin, Blut 30 (1975) 121–134.

[7] B. Sweryda-Krawiec, H. Devaraj, G. Jacob, J.J. Hickman, A new interpretation of serum albumin surface passivation, Langmuir 20 (2004) 2054–2056.
[8] Y. Xiao, S.N. Isaacs, Enzyme-linked immunosorbent assay (ELISA) and blocking with bovine serum albumin (BSA)—Not all BSAs are alike, J. Immunol. Methods 384 (2012) 148–151.
[9] J.N. Belling, J.A. Jackman, S. Yorulmaz Avsar, J.H. Park, Y. Wang, M.G. Potroz, A.R. Ferhan, P.S. Weiss, N.-J. Cho, Stealth immune properties of graphene oxide enabled by surface-bound complement Factor H, ACS Nano 10 (2016) 10161–10172.
[10] W. Norde, Adsorption of proteins from solution at the solid-liquid interface, Adv. Colloid Interface Sci. 25 (1986) 267–340.
[11] M. Karlsson, J. Ekeroth, H. Elwing, U. Carlsson, Reduction of irreversible protein adsorption on solid surfaces by protein engineering for increased stability, J. Biol. Chem. 280 (2005) 25558–25564.
[12] T. Peters Jr, Serum albumin, Adv. Protein Chem. Elsevier, 1985, pp. 161–245.
[13] D.C. Carter, J.X. Ho, Structure of serum albumin, Adv. Protein Chem. Elsevier, 1994, pp. 153–203.
[14] S. Sugio, A. Kashima, S. Mochizuki, M. Noda, K. Kobayashi, Crystal structure of human serum albumin at 2.5 Å resolution, Protein Eng. 12 (1999) 439–446.
[15] A. Bujacz, Structures of bovine, equine and leporine serum albumin, Acta Crystallogr. Sect. D: Biol. Crystallogr. 68 (2012) 1278–1289.
[16] A. Bujacz, J.A. Talaj, K. Zielinski, A.J. Pietrzyk-Brzezinska, P. Neumann, Crystal structures of serum albumins from domesticated ruminants and their complexes with 3, 5-diiodosalicylic acid, Acta Crystallogr. Sect. D: Struct. Biol. 73 (2017) 896–909.
[17] J. Steinhardt, J. Krijn, J.G. Leidy, Differences between bovine and human serum albumins. Binding isotherms, optical rotatory dispersion, viscosity, hydrogen ion titration, and fluorescence effects, Biochemistry 10 (1971) 4005–4015.
[18] J. Masuoka, P. Saltman, Zinc (II) and copper (II) binding to serum albumin. A comparative study of dog, bovine, and human albumin, J. Biol. Chem. 269 (1994) 25557–25561.
[19] T. Kosa, T. Maruyama, M. Otagiri, Species differences of serum albumins: I. Drug binding sites, Pharm. Res. 14 (1997) 1607–1612.
[20] I. Fitos, J. Visy, M. Simonyi, Species-dependency in chiral-drug recognition of serum albumin studied by chromatographic methods, J. Biochem. Biophys. Methods 54 (2002) 71–84.
[21] M. Pistolozzi, C. Bertucci, Species-dependent stereoselective drug binding to albumin: a circular dichroism study, Chirality 20 (2008) 552–558.
[22] X.-L. Han, F.-F. Tian, Y.-S. Ge, F.-L. Jiang, L. Lai, D.-W. Li, Q.-L. Yu, J. Wang, C. Lin, Y. Liu, Spectroscopic, structural and thermodynamic properties of chlorpyrifos bound to serum albumin: a comparative study between BSA and HSA, J. Photochem. Photobiol. B 109 (2012) 1–11.
[23] M. Poór, Y. Li, G. Matisz, L. Kiss, S. Kunsági-Máté, T. Kőszegi, Quantitation of species differences in albumin–ligand interactions for bovine, human and rat serum albumins using fluorescence spectroscopy: a test case with some Sudlow's site I ligands, J. Lumin. 145 (2014) 767–773.
[24] S. Ketrat, D. Japrung, P. Pongprayoon, Exploring how structural and dynamic properties of bovine and canine serum albumins differ from human serum albumin, J. Mol. Graphics Modell. (2020) 107601.
[25] T. Kosa, T. Maruyama, M. Otagiri, Species differences of serum albumins: II. Chemical and thermal stability, Pharm. Res. 15 (1998) 449–454.
[26] C.B. Bleustein, M. Sennett, R.T. Kung, D. Felsen, D.P. Poppas, R.B. Stewart, Differential scanning calorimetry of albumin solders: interspecies differences and fatty acid binding effects on protein denaturation, Lasers Surg. Med. 27 (2000) 465–470.
[27] A. Michnik, K. Michalik, A. Kluczewska, Z. Drzazga, Comparative DSC study of human and bovine serum albumin, J. Therm. Anal. Calorim. 84 (2005) 113–117.
[28] E. Ahmad, P. Sen, R.H. Khan, Structural stability as a probe for molecular evolution of homologous albumins studied by spectroscopy and bioinformatics, Cell Biochem. Biophys. 61 (2011) 313–325.
[29] R. Kurrat, J. Prenosil, J. Ramsden, Kinetics of human and bovine serum albumin adsorption at silica–titania surfaces, J. Colloid Interface Sci. 185 (1997) 1–8.
[30] Y. Mao, W. Wei, H. Peng, J. Zhang, Monitoring for adsorption of human serum albumin and bovine serum albumin onto bare and polystyrene-modified silver electrodes by quartz crystal impedance analysis, J. Biotechnol. 89 (2001) 1–10.
[31] M. Iafisco, P. Sabatino, I.G. Lesci, M. Prat, L. Rimondini, N. Roveri, Conformational modifications of serum albumins adsorbed on different kinds of biomimetic hydroxyapatite nanocrystals, Colloids Surf. B 81 (2010) 274–284.
[32] M. Voicescu, S. Ionescu, D.G. Angelescu, Spectroscopic and coarse-grained simulation studies of the BSA and HSA protein adsorption on silver nanoparticles, J. Nanopart. Res. 14 (2012) 1174.
[33] L. Bekale, D. Agudelo, H. Tajmir-Riahi, Effect of polymer molecular weight on chitosan–protein interaction, Colloids Surf. B 125 (2015) 309–317.
[34] R.E. Cristian, I.J. Mohammad, M. Mernea, B.G. Sbarcea, B. Trica, M.S. Stan, A. Dinischiotu, Analyzing the interaction between two different types of nanoparticles and serum albumin, Materials 12 (2019) 3183.
[35] G.J. Ma, A.R. Ferhan, J.A. Jackman, N.-J. Cho, Quantitative Assessment of Bovine Serum Albumin Proteins for Blocking Applications, bioRxiv, 2019869677.
[36] J.H. Park, A.R. Ferhan, J.A. Jackman, N.-J. Cho, Modulating conformational stability of human serum albumin and implications for surface passivation applications, Colloids Surf. B 180 (2019) 306–312.
[37] C.N. Pace, F. Vajdos, L. Fee, G. Grimsley, T. Gray, How to measure and predict the molar absorption coefficient of a protein, Protein Sci. 4 (1995) 2411–2423.
[38] N.-J. Cho, C.W. Frank, B. Kasemo, F. Höök, Quartz crystal microbalance with dissipation monitoring of supported lipid bilayers on various substrates, Nat. Protoc. 5 (2010) 1096.
[39] J.A. Jackman, V.P. Zhdanov, N.-J. Cho, Nanoplasmonic biosensing for soft matter adsorption: kinetics of lipid vesicle attachment and shape deformation, Langmuir 30 (2014) 9494–9503.
[40] G.H. Zan, J.A. Jackman, S.O. Kim, N.J. Cho, Controlling lipid membrane architecture for tunable nanoplasmonic biosensing, Small 10 (2014) 4828–4832.
[41] S.S. Strickler, A.V. Gribenko, A.V. Gribenko, T.R. Keiffer, J. Tomlinson, T. Reihle, V.V. Loladze, G.I. Makhatadze, Protein stability and surface electrostatics: a charged relationship, Biochemistry 45 (2006) 2761–2766.
[42] U. Kragh-Hansen, S. Saito, K. Nishi, M. Anraku, M. Otagiri, Effect of genetic variation on the thermal stability of human serum albumin, Biochim. Biophys. Acta Proteins Proteomics 1747 (2005) 81–88.
[43] J.H. Park, J.A. Jackman, A.R. Ferhan, G.J. Ma, B.K. Yoon, N.-J. Cho, Temperature-induced denaturation of BSA protein molecules for improved surface passivation coatings, ACS Appl. Mater. Interfaces 10 (2018) 32047–32057.
[44] F.J. Mannuzza, J.G. Montalto, Is bovine albumin too complex to be just a commodity? Bioprocess Int. 8 (4) (2010) 42–49.
[45] G. Zazeri, A.P.R. Povinelli, Md.F. Lima, M.L. Cornélio, Experimental approaches and computational modeling of rat serum albumin and its interaction with piperine, Int. J. Mol. Sci. 20 (2019) 2856.
[46] J.A. Jackman, A.R. Ferhan, N.-J. Cho, Nanoplasmonic sensors for biointerfacial science, Chem. Soc. Rev. 46 (2017) 3615–3660.
[47] J.A. Jackman, A.R. Ferhan, B.K. Yoon, J.H. Park, V.P. Zhdanov, N.-J. Cho, Indirect nanoplasmonic sensing platform for monitoring temperature-dependent protein adsorption, Anal. Chem. 89 (2017) 12976–12983.
[48] A.R. Ferhan, J.A. Jackman, T.N. Sut, N.-J. Cho, Quantitative comparison of protein adsorption and conformational changes on dielectric-coated nanoplasmonic sensing arrays, Sensors 18 (2018).
[49] J.A. Jackman, S. Yorulmaz Avsar, A.R. Ferhan, D. Li, J.H. Park, V.P. Zhdanov, N.-J. Cho, Quantitative profiling of nanoscale liposome deformation by a localized surface plasmon resonance sensor, Anal. Chem. 89 (2017) 1102–1109.
[50] R. Nord, J.W. Evans, Irreversible immobile random adsorption of dimers, trimers,… on 2 D lattices, J. Chem. Phys. 82 (1985) 2795–2810.
[51] J.J. Gillissen, J.A. Jackman, S.R. Tabaei, N.-J. Cho, A numerical study on the effect of particle surface coverage on the quartz crystal microbalance response, Anal. Chem. 90 (2018) 2238–2245.
[52] K.K. Chittur, FTIR/ATR for protein adsorption to biomaterial surfaces, Biomaterials 19 (1998) 357–369.